Mutation of TweedleD, a member of an unconventional cuticle protein family, alters body shape in *Drosophila*

Xiao Guan, Brooke W. Middlebrooks, Sherry Alexander, and Steven A. Wasserman*

Section of Cell and Developmental Biology, University of California at San Diego, 9500 Gilman Drive, La Jolla, CA 92093-0349

Communicated by Dan L. Lindsley, University of California at San Diego, La Jolla, CA, September 6, 2006 (received for review July 17, 2006)

Body shape determination represents a critical aspect of morphogenesis. In the course of investigating body shape regulation in *Drosophila*, we have identified a dominant mutation, *TweedleD*^{1} (*TwdlD*^{1}), that alters overall dimensions at the larval and pupal stages. Characterization of the affected locus led to the discovery of a gene family that has 27 members in *Drosophila* and is found only among insects. Analysis of gene expression at the RNA and protein levels revealed gene-specific temporal and spatial patterns in ectodermally derived tissues. In addition, light microscopic studies of fluorescently tagged proteins demonstrated that Tweedle proteins are incorporated into larval cuticular structures. This demonstration that a mutation in a *Drosophila* cuticular protein gene alters overall morphology confirms a role for the fly exoskeleton in determining body shape. Furthermore, parallels between these findings and studies of cuticle collagen genes in *Caenorhabditis elegans* suggest that the exoskeleton influences body shape in diverse organisms.

arthropod | morphogenesis | tandem duplication | Tubby

Morphogenesis into a viable adult animal relies on developmental regulation of size and shape. In *Drosophila*, body size and body shape are controlled by correlated but distinct activities. For example, antagonistic cross-talk between the ecdysone and insulin signaling pathways regulates the final size of an individual fly without any accompanying variation in body shape (1). Furthermore, there are mutations that impart a short and wide body shape on larvae and adults but do not alter body mass. Although shaping processes such as convergent extension have been intensively studied in recent years (2, 3), there has been no broad investigation of shape-determining activities in the fruit fly.

The most extensive studies of body shape determination have been carried out with the nematode *Caenorhabditis elegans*. More than 50 *C. elegans* mutations that affect overall morphology have been described. Their phenotypes vary widely, as is apparent in characterizations that include blister, dumpy, and long, as well as left- and right-handed roller (4). Many of these mutations have been mapped, and the affected genes have been identified. More than half the mutations altering worm body shape (specifically the dumpy and long mutations) map to genes that encode cuticle collagens, the major components of the worm cuticle (5). Of those mutations causing a dumpy phenotype, a number disrupt the function of collagen-modifying enzymes, including prolyl-4-hydroxylases, a protein disulfide isomerase, and a procollagen C-proteinase (6–10). These data point to the structure of the exoskeleton as being a major factor in determining the overall shape of individual worms.

Like worms, fruit flies rely on a cuticular exoskeleton. However, whereas *C. elegans* has >170 cuticle collagen genes, *Drosophila* has very few genes encoding collagen molecules (4). Furthermore, none of the encoded collagens closely resembles the worm cuticle forms. The *Drosophila* cuticle is a stratified structure comprising an envelope layer, a proteinaceous epicuticle, and a procuticle rich in chitin (polymer of *N*-acetylglucosamine) (11). The envelope functions as a support for subsequent cuticle deposition, and the epicuticle and the procuticle together stiffen the exoskeleton. The chitin microfibrils and associated proteins in the procuticle form a characteristic lamella, which is crucial for maintaining cuticle tension. In contrast, the epicuticle is composed of a large number of proteins (estimated in the hundreds) (12), which are cross-linked through sclerotization or melanization (13).

Mutations in *Drosophila* that disrupt the synthesis, modification, or deposition of chitin have been identified for a number of loci, including the genes for chitin synthase (*kkv*), UDP-*N*-acetylglucosamine pyrophosphorylase (*mummy*), and chitin-modifying proteins (*serpentine*, *vermiform*, *knickkopf*, and *retroactive*) (14–21). In each case, gene inactivation results in a dilated or deformed cuticle. For example, loss-of-function mutations in *knickkopf* or *retroactive* disrupt the structure of the lamella, leading to a loss of cuticle integrity and a bloated embryo appearance (20).

Mutations of a number of genes outside the chitin metabolic pathways alter body shape in flies. For instance, a recessive, hypomorphic allele of Calmodulin (*Cam*^{7}) results in a squat pupal shape (22). There is evidence that the squat shape results from a hypercontraction of body wall muscle during pupariation, the larval–pupal transition. Similarly, a failure of muscles to contract properly during pupariation is thought to explain the extended, or twiggy, shape of pupae mutant for Mlp84B, a gene that encodes a muscle-specific LIM protein (K. A. Clark, personal communication). Alteration of body shape has also been observed for mutations in Toll pathway components (ref. 23 and S.A.W., unpublished results). Loss of function for Toll, Myd88, Tube, or Pelle causes a squat pupal shape, whereas inactivation of the inhibitor Cactus results in an elongated body shape. The exact relationship between Toll pathway function and body shape determination is unknown, but it may reflect the requirement for Toll in patterning and innervation of the larval musculature (24).

To further explore body shape determination in *Drosophila*, we conducted a genetic screen for dominant, radiation-induced mutations that cause a squat or twiggy pupal body shape. Among those identified was a mutation resulting in a body that is both shorter and wider than wild type. Characterization of the affected gene has provided insight into the role of a previously unrecognized gene family of cuticle components.

Results

The *TweedleD*^{1} Mutation Alters Body Shape in Larvae and Pupae. During larval and pupal stages, the body shape of a fly can be conveniently described by the axial ratio (A.R., length/width) of

Author contributions: X.G., S.A., and S.A.W. designed research; X.G., B.W.M., and S.A. performed research; X.G., B.W.M., and S.A. contributed new reagents/analytic tools; X.G., S.A., and S.A.W. analyzed data; and X.G. and S.A.W. wrote the paper.

The authors declare no conflict of interest.

Abbreviations: RFP, red fluorescent protein; A.R., axial ratio.

*To whom correspondence should be addressed. E-mail: stevenw@ucsd.edu.

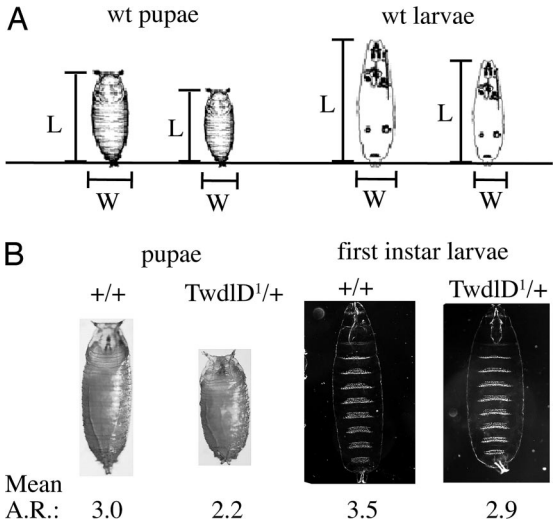

Fig. 1. Quantitation of the squat phenotype by A.R. (*A*) The body shape of a pupa or larva can be described by the length/width A.R. of its cuticle. (*B*) The *TwdlD*^{1} mutation reduces the mean A.R. of pupae and larvae. Number of individuals measured: 20 for larvae and 40 for pupae. Standard deviation = 0.1.

its cuticle. Experiments done in our laboratory (23) have demonstrated that flies of a particular genetic background have a fixed mean A.R. despite differences in size caused by nutrition and population density (Fig. 1*A*). The mean pupal A.R. of the commonly used wild-type strain *Oregon R*, as well as w^{1118}, is 3.0 ± 0.1 (Fig. 1*B*).

The *TweedleD*^{1} (*TwdlD*^{1}) mutation has a dramatic effect on body shape, resulting in a squat body shape and reducing the A.R. to just 2.2 ± 0.1(Fig. 1*B*). Both the width and the length of the pupal case are affected, although the change in length is more readily apparent by inspection. The reduction in A.R. is similar for heterozygotes and homozygotes. Adults appear slightly more squat than wild type. Viability and fertility are unaffected.

Because the *TwdlD*^{1} phenotype was readily detectable in older (second- and third-instar) larvae, we were interested in determining whether embryonic and early larval development might also be affected. We collected newly hatched first-instar larvae, generated flattened cuticle preparations, and measured overall body dimensions. To ensure that we were looking at only zygotic effects, we generated *TwdlD*^{1} heterozygotes by crossing wild-type females to *TwdlD*^{1}/*TwdlD*^{1} males. The cuticles of young wild-type first instars had an A.R. of 3.5 ± 0.1 (Fig. 1*B*). In contrast, the cuticles of *TwdlD*^{1}/+ larvae had an A.R. of only 2.9 ± 0.1. The effects of the *TwdlD*^{1} mutation on body shape are thus apparent from at least the end of embryogenesis through the pupal stage.

Overall, the phenotype of the *TwdlD*^{1} mutation is very similar to that of a previously described mutation, *Tubby*^{1} (*Tb*^{1}). (The *Tb* locus was named for the mutant phenotype and does not correspond to either *Drosophila* homolog of the mammalian Tubby gene.) As with *TwdlD*^{1}, the *Tb*^{1} mutation reduces the A.R. in a dominant fashion without affecting viability or fertility. At the pupal stage, we find that *Tb*^{1} results in an A.R. of 2.0 ± 0.1, a slightly more severe effect than was seen with *TwdlD*^{1}. Like *TwdlD*^{1}, *Tb*^{1} results in a heterozygous phenotype that is indistinguishable from that of homozygous mutants. Furthermore, we localized *TwdlD* by meiotic recombination mapping to position 3–91, where *Tb* had previously been mapped (25).

The TweedleD Locus Encodes a Member of an Insect-Specific Gene Family. To initiate a molecular characterization of the *TweedleD* and *Tubby* loci, we carried out fine-structure mapping by *P*-element-induced male recombination (26). The meiotic map position 3–91 corresponds to the region surrounding polytene band 97C on the right arm of the third chromosome. We therefore used six *P* insertion lines within the region 97B9–D3 to map *TwdlD*^{1} and *Tb*^{1} (Fig. 2). Both mutations mapped to the 73.8-kb interval proximal to the gene *amontillado*. We sequenced genomic DNA spanning this 73.8-kb region for *Tb*^{1} homozygotes, *TwdlD*^{1} homozygotes, and the parental strain from which *TwdlD*^{1} was derived (the parental strain for *Tb*^{1} was not available). Initial sequencing of *Tb*^{1} revealed a high density of sequence alterations relative to the published genomic sequence. For *TwdlD*^{1}, however, we found a single sequence change relative to the parental strain: a 9-nt deletion in the published sequence for CG14243, an uncharacterized gene.

The TweedleD protein encoded by CG14243 contains 256 aa. Examination of the predicted *D. melanogaster* proteome reveals 26 homologues of TwdlD. Overall sequence identity to TwdlD ranges from 26% to 54%. Of the 27 related genes, which we have termed the Tweedle family, TwdlD and 21 others are distributed among three gene clusters: one on the X chromosome (polytene band 15A3) and two on the third chromosome (polytene bands 82A1 and 97C). Each of the 27 family members is predicted to contain an N-terminal signal peptide, but not a transmembrane domain.

To determine whether Tweedle family members are secreted, we expressed epitope-tagged forms of TwdlD and TwdlJ (CG5471) in cultured *Drosophila* S2 cells. For both genes, the vast majority of the tagged protein was found in the culture media (Fig. 3), demonstrating that the polypeptides are indeed being secreted.

Using the TwdlD amino acid sequence to search translated forms of animal and plant genomes, we identified two or more Tweedle family members in all insects examined, but none in any other species, including *Daphnia*, a crustacean. Alignment of protein sequences from *Drosophila*, *Anopheles*, *Aedes*, *Bombyx*,

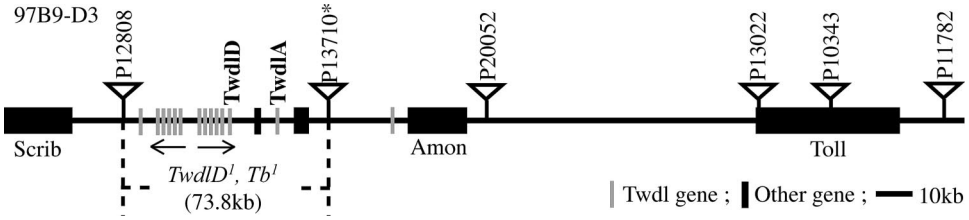

Fig. 2. The gene CG14243 is mutated in the *TwdlD*^{1} mutant. *TwdlD*^{1} and *Tb*^{1} were mapped by *P* element-induced male recombination within the polytene interval 97B9–D3 (inverted triangles indicate *P* element insertions). Both mutations mapped to a 73.8-kb region distal to *scribble* (*scrib*) and proximal to *amontillado* (*amon*). Two sets of genes within this region were tandemly arrayed with regard to transcription (arrows). Sequencing of the *TwdlD*^{1} mutant identified a 9-bp deletion in the coding region of gene CG14243 (TwdlD). The location shown for P13710 (asterisk) reflects an ≈25-kb deletion on the proximal side of the original insertion site generated during *P*-mediated recombination. The Twdl genes (gray bars) in the region are, from left to right, TwdlM, TwdlP, TwdlB, TwdlL, TwdlO, TwdlK, TwdlJ, TwdlN, TwdlH, TwdlR, TwdlS, TwdlD, and TwdlA.

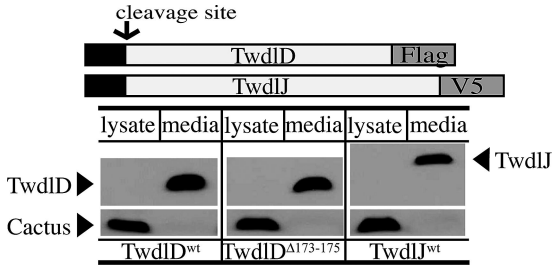

Fig. 3. TwdlD and its homologue TwdlJ encode secreted proteins. S2 cells were transfected with constructs expressing Flag-tagged TwdlD^{wt} or TwdlD$^{\Delta 173-175}$, or with V5-tagged TwdlJ^{wt}. Media and cell pellets were separated by centrifugation, and equivalent amounts of media and total cell lysate were resolved by SDS/PAGE for immunoblotting. Proteins were detected with antibodies specific for their epitope tags. Blotting of a replicate gel with rabbit antiserum against Cactus, a cytoplasmic protein, controlled for separation of intact cells from media.

Apis, and *Tribolium* revealed several well conserved blocks (Fig. 4). None comprises a previously described motif. The positions of highly conserved amino acids within these blocks strongly suggest the presence of an internal repeat structure in each family member. In particular, blocks I and III contain a motif of the form $KX_{2-3}YV$ (where X_{2-3} represents two or three nonconserved amino acids), whereas blocks II and IV contain a $KX_{4-5}FIK$ motif. Furthermore, a secondary structure calculation made with the PHD program predicts a β-strand conformation for each of the four blocks (Fig. 4).

The region most conserved among all of the family members is that defined by an extended motif that spans the conserved block III and IV: $YVLX_{20-23}$KPEVyFiKY(R/K)t, where lowercase letters represent less strict conservation. Strikingly, the 9-bp deletion caused by the *TwdlD^1* mutation maps to this motif, eliminating the tripeptide KYR at positions 173–175 in the TwdlD protein and the block IV. Consistent with the dominant nature of the Δ173–175 mutation, loss of these residues has no detectable effect on secretion or stability of the TwdlD protein (Fig. 3).

To substantiate that the Δ173–175 deletion in *TwdlD^1* underlies the dominant squat phenotype, we carried out germ-line transformation experiments. Wild-type and Δ173–175 forms of TwdlD were placed in a transformation vector downstream of the presumptive TwdlD promoter. We examined four independent transgenic lines for wild-type TwdlD; pupae from each exhibited a normal A.R. In contrast, pupae from each of three

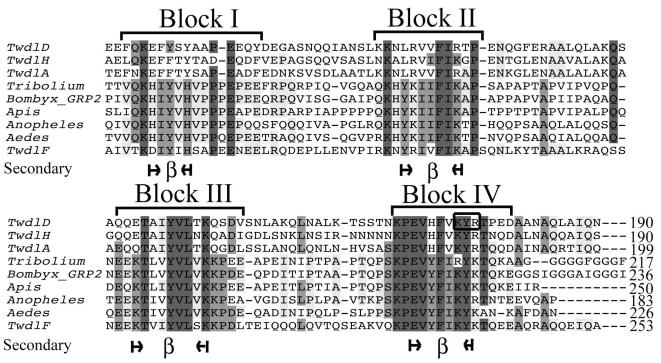

Fig. 4. Alignment of Tweedle family protein sequences. Amino acids are colored to reflect percent identity among the nine sequences: dark gray, conserved in eight or nine; medium gray, conserved in six or seven; light gray, conserved in four or five. The four β-strands predicted with the PHD program are shown. The amino acids KYR deleted in *TwdlD^1* are boxed.

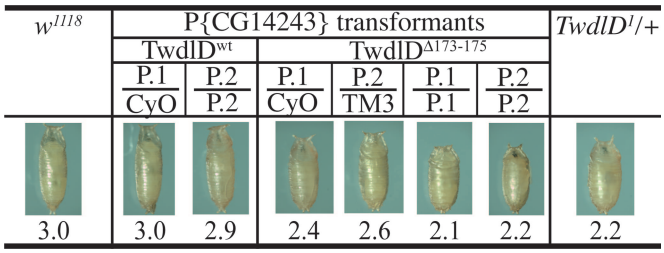

Fig. 5. Exogenous expression of TwdlD$^{\Delta 173-175}$ causes the *TwdlD^1* phenotype in transgenic flies. Numbers at bottom are mean A.R. derived from measurements of 40 pupae from each line. The standard deviation of the mean A.R. was 0.1 in all cases. For each construct, P.1 and P.2 represent a pair of independent isolates.

independent lines for TwdlD$^{\Delta 173-175}$ had a readily observable squat phenotype (Fig. 5). These findings demonstrate that the 3-aa deletion in TwdlD is responsible for the dominant phenotype of the *TwdlD^1* allele.

In characterizing the transgenic pupae, we noted that two copies of the Δ173–175 transgene had a greater effect on body shape than a single copy. In particular, pupae carrying two copies of the mutant transgene had a mean A.R. of 2.1–2.2, similar to *TwdlD^1* pupae, whereas those with a single copy had an A.R. of ≈2.5, intermediate between wild-type and *TwdlD^1*. Because there are two wild-type copies of TwdlD in the genetic background for the transgene experiments, these results suggest that the most severe phenotype is expressed only when the ratio of the mutant to the wild-type gene is 1:1 or greater.

TwdlD belongs to the 97C Twdl gene cluster, which includes 13 of the 15 annotated genes in the 73.8-kb region within which *TwdlD^1* and *Tb^1* map. To determine whether *Tb^1*, like *TwdlD^1*, mutates a Tweedle family member, we examined the *Tb^1* genomic sequence for changes in the coding sequence of Tweedle genes. By this means, we found a deletion that removes residues 167–190 in the coding region of TwdlA (CG5480) (Fig. 4). This change eliminates all of block IV, as well as the linker between blocks III and IV, from TwdlA. Given the similarity of the TwdlA Δ167–190 deletion in *Tb^1* to the Δ173–175 mutation in *TwdlD^1*, we propose that this change in TwdlA is responsible for the *Tb^1* phenotype.

A New Family of Fly Cuticle Proteins. The observation that the *TwdlD^1* phenotype was apparent in newly hatched first-instar larvae provided good evidence for embryonic expression of TwdlD. To determine when and where TwdlD is expressed, and whether distinct family members differ in their expression patterns, we carried out *in situ* hybridization in embryos. For all seven of the genes tested, transcripts were detected at embryonic stages 13–16 (Fig. 6), but not earlier (data not shown). Expression of TwdlD, as well as TwdlB (CG6478) and TwdlF (CG14639), was detected within the epidermis, with the expression of TwdlD and TwdlB forming segmental stripes along the anteroposterior axis. In contrast, the transcripts of the remaining loci were each found in a more restricted domain of the embryo: the tracheal tree [Twdlβ (CG8986)], dorsal epidermis (TwdlA), and the foregut [TwdlC (CG14254) and TwdlE (CG14534)]. Although the patterns were varied, expression of all family members tested was confined to tissues that are ectodermal in origin.

Theoretically, an alteration in body shape could result from various causes, including neuronal malfunction, defective musculature, or structural abnormalities of the integument. To delimit the biological functions most likely affected by the *TwdlD^1* mutation, we designed experiments to monitor wild-type patterns of protein expression for TwdlD and two other family

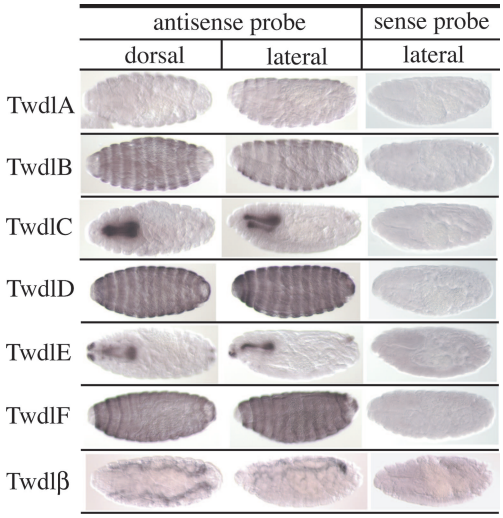

Fig. 6. Tweedle family genes are expressed in the hypodermis, foregut, or tracheal system of late-stage embryos. RNA expression of genes TwdlA–TwdlF as well as Twdlβ was examined by *in situ* hybridization with antisense probes. All embryos are arranged with anterior to the left. Both dorsal (*Left*) and lateral (*Center*) embryo aspects are presented for each gene. A lateral (*Right*) view of embryos probed with sense strand control is also presented.

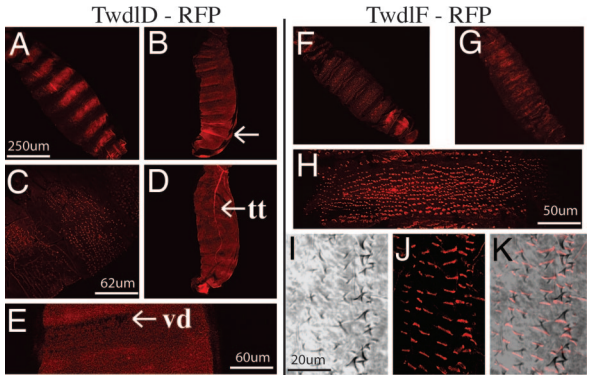

Fig. 8. Genes TwdlD and TwdlF encode cuticular proteins. Fixed first-instar larvae (2 h) were observed by confocal microscopy. (*A*) The TwdlD–RFP fusion protein forms 10 stripes on the integument along the AP axis. (*B*) The TwdlD–RFP protein is incorporated into the cuticle structure. The arrow in *B* shows a site where the larval body is detached from the cuticle. (*C*) TwdlD–RFP fluorescence is apparent in cuticular dorsal hairs. (*D*) The TwdlD–RFP protein is incorporated into the tracheal system. (*E*) The ventral denticles are not fluorescent in the TwdlD–RFP transgenics. (*F* and *G*) The TwdlF–RFP fusion protein is detectable within the cuticle. (*H*) TwdlF–RFP fluorescence in dorsal hairs. (*I–K*) TwdlF–RFP fluorescence in ventral denticles is confined to the basal portion. A differential interference contrast image (*I*), an RFP image (*J*), and a merged image (*K*) are presented. *tt*, tracheal tree; *vd*, ventral denticle.

members. We generated fusion protein constructs in which sequences encoding monomeric red fluorescent protein (RFP) were introduced immediately 3′ to the coding regions of TwdlD, TwdlF, and TwdlH (CG31080). Each construct retained endogenous sequences representing the promoter, as well as the 5′ and 3′ UTR. Independent transgenic lines were generated by *P* element-mediated transformation.

The three family members exhibited distinct temporal and spatial localization patterns (Fig. 7). Expression of the TwdlD–RFP fusion protein was strongest during the first and the second larval instars. During these stages, TwdlD was detectable in the integument, as well as the tracheal tree (Figs. 7 and 8*D*). Signal in the integument was detected in 10 transverse stripes distributed along the anteroposterior axis. Expression in the integument was in fact cuticular, as demonstrated by the appearance of fluorescent signal within the cuticular structures known as dorsal hairs (Fig. 8*C*). Furthermore, that the striped expression pattern was associated with cuticle was apparent from examination of larvae in which the cuticle had been detached from the larval body during fixation and preparation (Fig. 8*B*). By the early third instar, TwdlD expression was largely limited to the anterior and the posterior tips of the larvae. By late in the third larval instar (wandering larva stage), fluorescent signal was no longer detected.

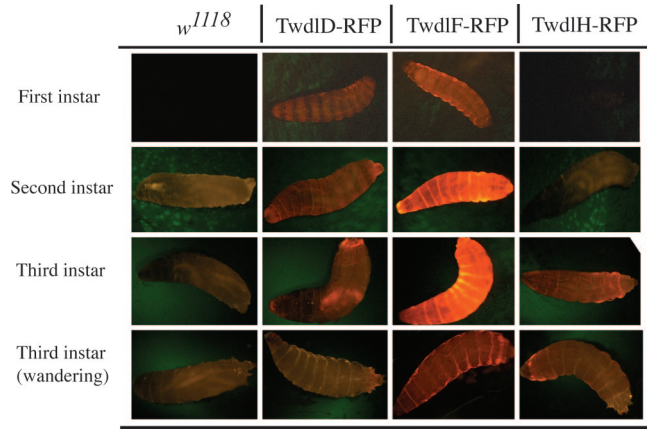

Fig. 7. Proteins of gene TwdlD, TwdlF, and TwdlH show a distinct temporal and spatial localization pattern. The location of each protein in the transgenic flies was monitored by means of the RFP tag fused to the C terminus. The TwdlD fusion protein is principally detectable during the first- and second-instar larval stages. The TwdlF fusion protein is identified in a fine layer of the integument through the whole larval stages. The TwdlH fusion protein is only visible in the third-instar larvae and within the segments close to the anterior or posterior ends.

As with TwdlD, the RFP fusions for TwdlF and TwdlH displayed a pronounced cuticular localization. In the case of TwdlF, the fusion protein was detected throughout larval development (Fig. 7). Fluorescence was associated with both dorsal hairs and ventral denticles (Fig. 8 *H* and *J*). For the ventral denticles, signal was for the most part limited to the basal portion, resulting in a narrow bar of expression parallel to the cuticular surface (Fig. 8 *I–K*). By comparison, TwdlH had a much more limited pattern of expression. The TwdlH–RFP fusion protein was detected only in third-instar larvae, where the signal was limited to the cuticle near the anterior and posterior ends (Fig. 7).

Although the three Tweedle proteins differ in the details of their expression patterns, all are cuticular proteins, consistent with a conserved role for the Tweedle family proteins in cuticle formation.

Discussion

The study of the *TwdlD*^{1} mutant has led us to the discovery of a protein family, the Tweedle family. We observe ectodermal expression for all family members tested. In addition, we have shown that at least three of the family members are cuticular proteins. Our findings thus establish a connection between body shape regulation and structural proteins that contribute to the cuticle.

Role of Tweedle Proteins in Cuticle Assembly. Insects have evolved the chitin-based cuticle to protect them from the environment. The *Drosophila* larval cuticle is secreted by the underlying hypodermis at its apical face, and a new cuticle is generated for

DEVELOPMENTAL BIOLOGY

each instar. The cuticle is attached to the hypodermis at multiple anchor sites (15). Extensive cross-linking is crucial in determining the mechanical properties of the cuticle. The *TwdlD*^{1} mutation, which does not change the stability or the secretion of the protein, is therefore very likely to affect either the conformation of the protein or its activity in forming or stabilizing cross-links.

The fact that the four most conserved blocks of amino acids in the Tweedle protein are predicted to form β-strands is intriguing. Previous studies of insect cuticle proteins have suggested that the barrel structure formed by multiple β-strands provides an interface for aromatic residues to stack with and bind to chitin (27, 28). In this regard, we note that several of the highly conserved residues in the Tweedle proteins that lie within these predicted β-strands have aromatic side chains: Y and H in block I, Y and F in block II, Y in block III and Y, and F and Y in block IV. We therefore postulate that the Twdl family proteins interact directly with chitin.

The Tweedle family members in the *Drosophila* genome form three major gene clusters. The 97C cluster, which includes the TwdlD gene, consists of 14 family members. This cluster can be furthered divided in half, with the genes in each half all being transcribed from the same DNA strand. Why has the Tweedle gene family apparently undergone multiple gene duplication events? Our studies indicate that the expansion in gene number was accompanied by a differentiation of distinct patterns of expression. One possibility, therefore, is that each family member functions identically at the biochemical level, with the differences in expression determining the organization of the cuticle. Thus, for example, different levels of Tweedle protein at particular locations could determine the extent of cross-linking and, hence, flexibility. Similarly, differences in the timing of expression could dictate the order of assembly of cuticle at distinct locations. Alternatively, family members could differ in biochemical function, with the sequence differences seen between family members dictating local differences in cuticle composition and properties.

Although none of the 27 Tweedle genes in *Drosophila* has been studied previously, a recent report describes a characterization of a related gene in the silkworm *Bombyx mori* (29). This silkworm protein, BmGRP2, was detected in the cuticle layer of the wing tissue and in the trachea in the silkworm. The authors noted that BmGRP2 contains a glycine-rich domain that is present in cuticle and other structural proteins in many species, where such domains are proposed to provide flexibility. We note, however, that BmGRP2 also contains a sequence with substantial similarity to the Tweedle family signature motif YVLX$_{20–23}$KPEVyFiKY(R/K)t (see Fig. 4).

Like BmGRP2, some Tweedle proteins contain glycine-rich domains. However, the glycine-rich domain is absent in 21 of the 27 *Tweedle* genes in *Drosophila*, including the three studied here at the protein level: TwdlD, TwdlF, and TwdlH. Furthermore, many glycine-rich cuticle proteins lack the motif conserved in the Tweedle family. For these reasons, we speculate that the Tweedle motif and the glycine-rich domain have distinct and largely independent functions in cuticle formation.

Genetic Control of Larval and Pupal Body Shape. Although the *TwdlD*^{1} phenotype is mostly easily recognized during the larval and the pupal stages, TwdlD gene expression begins in the latter half of embryogenesis (see Fig. 6) and is no longer detectable by the end of the last larval stage. The lack of any shape alteration in *TwdlD*^{1} embryos (data not shown) presumably reflects the fact that the surrounding eggshell is a protein-based extracellular matrix distinct from cuticle (30). Within the eggshell, however, the embryonic cuticle structure is clearly affected, as is evident upon examination of newly hatched first-instar larvae (see Fig. 1). A strong *TwdlD*^{1} phenotype observed during the pupal stage, after the cessation of gene expression, very likely represents residual effects during pupariation of the larval cuticle abnormality.

Two previously described dominant mutations, *Tubby*^{1} (*Tb*^{1}) and *Kugel*^{Valencia} (*Kg*^{V}), have phenotypes highly reminiscent of *TwdlD*^{1}. Like *TwdlD*^{1}, these mutations reduce A.R. at the larval and pupal stages. This similarity suggests that the three loci may act in the same pathway. We have mapped *Tb*^{1} to the same 73.8-kb region as *TwdlD*^{1} by *P*-induced male recombination, and we found a deletion within TwdlA that is the likely cause of the *Tb*^{1} phenotype. In the case of *Kg*^{V}, the mutation maps to the left side of the gene *Ki*, which is positioned at 83D–E on the polytene map. Although the mapping is less precise than that for *Tb*^{1}, this position is also roughly coincident with the location of a Tweedle gene cluster, the four Tweedle genes at 82A. We consider it very likely, therefore, that a mutation in this gene cluster is mutated in the *Kg*^{V} mutant.

People have known for a long time that the disruption of normal cuticle structure in *C. elegans* can cause the dumpy phenotype, which describes the shorter and wider morphology of the mutant worms. We have demonstrated in this report that the *TwdlD*^{1} mutation of the cuticular protein TwdlD causes a similar morphology change in the fruit fly. The analogy between the two systems highlights the importance of a cuticle in maintaining the wild-type body shape in organisms with an exoskeleton.

Materials and Methods

Genetic Screen for Morphology Mutations. To screen for dominant mutations on the third chromosome affecting pupal shape, we crossed mutagenized males (4,000-rad γ-irradiation) to virgin females and assayed directly for altered A.R. in pupae (see below). From ≈25,400 pupae, we identified two stable dominant mutations and characterized one, designated *TweedleD*^{1}.

Axial Ratio Determination. For pupae, A.R. (length/width) was measured by using a reticle in a stereo light microscope. For each genotype we measured at least 40 individuals and calculated the mean A.R. For larvae, A.R. was determined from digital photographs of cuticle preparations. At least two independent preparations were examined for each genotype, and 20 individual cuticles were measured for each preparation.

***P*-Induced Male Recombination Mapping.** *P* element-induced male recombination mapping was performed as described (26). Triply labeled chromosomes *Ly Tb*^{1} *Dr* and *e TwdlD*^{1} *Dr* were generated by meiotic recombination. *P* insertion lines BL12808, BL13710, BL20052, BL13022, BL10343, and BL11782 were obtained from Bloomington Stock Center (Bloomington, IN).

Sequence Analysis and Gene Assignments. Similarity searches used BLAST (www.ncbi.nlm.nih.gov/BLAST). The multiple protein alignment and similarity analysis were carried out by using CLUSTALW (www.ebi.ac.uk/clustalw). Detailed information on gene assignments for Tweedle family members is provided in *Supporting Materials and Methods* and Table 1, which are published as supporting information on the PNAS web site. The signal peptide prediction was made by using SignalP 3.0 (www.cbs.dtu.dk/services/SignalP) (31). Secondary structures were predicted with the PHD algorithm (32) (www.predictprotein.org) (33).

Protein Expression in S2 Cell Culture. The TweedleD coding region was fused to a FLAG tag at its C terminus and cloned into the pAc5.1/V5-His A vector (Invitrogen, Carlsbad, CA). The TweedleJ coding region was cloned into the same vector, where it was fused to the V5 epitope tag. S2 cell transfection and protein extract harvesting were as described (*Drosophila* Expression System; Invitrogen). For each plate of transfected cells, the media and the cell pellet were separated by centrifugation at 850 × *g*, and a 1/60th volume of the media and of the total cell lysate was each loaded

onto an SDS/PAGE gel for immunoblotting. Antibodies used in this experiment were as follows: anti-V5 antibody at 1:10,000 dilution (46-0705; Invitrogen), anti-FLAG M2 antibody at 1:1,000 dilution (200472-2; Stratagene, La Jolla, CA), and rabbit anti-Cactus antiserum at 1:10,000 dilution (34).

Embryonic *in Situ* Hybridization. Embryonic RNA expression patterns were investigated by *in situ* hybridization. The 3′ UTRs of target genes were amplified from the w^{1118} genome by PCR and cloned into the pBluescript vector (Stratagene). Digoxigenin-11-UTP was incorporated into sense and antisense probes generated with T7 and T3 RNA polymerase, respectively. Alkaline phosphatase-conjugated anti-digoxigenin antibody (Fab fragments; Roche, Pleasanton, CA) was used at a 1:2,000 dilution.

RFP Constructs, Transgenic Flies, and Microscopy. Tweedle gene genomic fragments including 500 bp of presumptive upstream regulatory sequence were cloned by PCR from the w^{1118} genome. We used PCR sewing (35) to fuse the 3′ end of each coding sequence in frame with sequences for the monomeric RFP DsRed (Clontech, Mountain View, CA). The resulting DNA fragments were ligated into the pCaSpeR transformation vector (36). Three independent transgenic lines were generated for each construct. Eggs were collected at 25°C for 2 h for each transgenic line and aged for 22, 48, or 72 h to obtain the young first-, second-, and third-instar larvae, respectively. Two-hour-old first-instar larvae were fixed as described (37) and observed under a confocal microscope.

Note. We have confirmed that *TwdlA* corresponds to the *Tubby* locus: Ten independent lines carrying a *TwdlA* transgene generated from Tb^1 have a squat pupal shape, whereas five lines carrying a *TwdlA* transgene from w^{1118} have a wild-type body shape.

We thank Dan Lindsley for helpful discussions; Jim Posakony (University of California at San Diego) for the transformation vector and RFP isoform used in these studies; Ethan Bier, Raffi Aroian, and Bill McGinnis for sharing microscopy facilities; and Ethan Bier for comments on the manuscript. This work was supported by National Institutes of Health Grant R01 GM50545 (to S.A.W.).

1. Colombani J, Bianchini L, Layalle S, Pondeville E, Dauphin-Villemant C, Antoniewski C, Carre C, Noselli S, Leopold P (2005) *Science* 310:667–670.
2. Keller R (2002) *Science* 298:1950–1954.
3. Ninomiya H, Elinson RP, Winklbauer R (2004) *Nature* 430:364–367.
4. Myllyharju J, Kivirikko KI (2004) *Trends Genet* 20:33–43.
5. Kramer JM, French RP, Park EC, Johnson JJ (1990) *Mol Cell Biol* 10:2081–2089.
6. Friedman L, Higgin JJ, Moulder G, Barstead R, Raines RT, Kimble J (2000) *Proc Natl Acad Sci USA* 97:4736–4741.
7. Myllyharju J, Kukkola L, Winter AD, Page AP (2002) *J Biol Chem* 277:29187–29196.
8. Winter AD, Page AP (2000) *Mol Cell Biol* 20:4084–4093.
9. Eschenlauer SC, Page AP (2003) *J Biol Chem* 278:4227–4237.
10. Novelli J, Ahmed S, Hodgkin J (2004) *Genetics* 168:1259–1273.
11. Payre F (2004) *Int J Dev Biol* 48:207–215.
12. Andersen SO, Hojrup P, Roepstorff P (1995) *Insect Biochem Mol Biol* 25:153–176.
13. Schaefer J, Kramer KJ, Garbow JR, Jacob GS, Stejskal EO, Hopkins TL, Speirs RD (1987) *Science* 235:1200–1204.
14. Ostrowski S, Dierick HA, Bejsovec A (2002) *Genetics* 161:171–182.
15. Moussian B, Schwarz H, Bartoszewski S, Nusslein-Volhard C (2005) *J Morphol* 264:117–130.
16. Moussian B, Soding J, Schwarz H, Nusslein-Volhard C (2005) *Dev Dyn* 233:1056–1063.
17. Araujo SJ, Aslam H, Tear G, Casanova J (2005) *Dev Biol* 288:179–193.
18. Tonning A, Helms S, Schwarz H, Uv AE, Moussian B (2006) *Development (Cambridge, UK)* 133:331–341.
19. Luschnig S, Batz T, Armbruster K, Krasnow MA (2006) *Curr Biol* 16:186–194.
20. Moussian B, Tang E, Tonning A, Helms S, Schwarz H, Nusslein-Volhard C, Uv AE (2006) *Development (Cambridge, UK)* 133:163–171.
21. Devine WP, Lubarsky B, Shaw K, Luschnig S, Messina L, Krasnow MA (2005) *Proc Natl Acad Sci USA* 102:17014–17019.
22. Wang B, Sullivan KM, Beckingham K (2003) *Genetics* 165:1255–1268.
23. Letsou A, Alexander S, Orth K, Wasserman SA (1991) *Proc Natl Acad Sci USA* 88:810–814.
24. Halfon MS, Hashimoto C, Keshishian H (1995) *Dev Biol* 169:151–167.
25. Lindsley DL (1973) *Drosophila Inf Serv* 50:21.
26. Chen B, Chu T, Harms E, Gergen JP, Strickland S (1998) *Genetics* 149: 157–163.
27. Hamodrakas SJ, Willis JH, Iconomidou VA (2002) *Insect Biochem Mol Biol* 32:1577–1583.
28. Iconomidou VA, Willis JH, Hamodrakas SJ (1999) *Insect Biochem Mol Biol* 29:285–292.
29. Zhong YS, Mita K, Shimada T, Kawasaki H (2006) *Insect Biochem Mol Biol* 36:99–110.
30. Fakhouri M, Elalayli M, Sherling D, Hall JD, Miller E, Sun X, Wells L, LeMosy EK (2006) *Dev Biol* 293:127–141.
31. Bendtsen JD, Nielsen H, von Heijne G, Brunak S (2004) *J Mol Biol* 340:783–795.
32. Rost B (1996) *Methods Enzymol* 266:525–539.
33. Rost B, Yachdav G, Liu J (2003) *Nucleic Acids Res* 32:W321–W326.
34. Reach M, Galindo RL, Towb P, Allen JL, Karin M, Wasserman SA (1996) *Dev Biol* 180:353–364.
35. Ho SN, Hunt HD, Horton RM, Pullen JK, Pease LR (1989) *Gene* 77: 51–59.
36. Thummel CS, Boulet AM, Lipshitz HD (1988) *Gene* 74:445–456.
37. Patel NH (1994) in *Drosophila melanogaster: Practical Uses in Cell and Molecular Biology*, eds Goldstein LSB, Fyrberg EA (Academic, San Diego), pp 455–461.